aerospace

MDPI

Article

Aircraft Configuration Parameter Boundaries Based on Closed-Loop Flying Qualities Requirements

Lixin Wang [1], Kun Yang [1], Peng Zhao [2] and Ting Yue [1,*]

[1] School of Aeronautic Science and Engineering, Beihang University, Beijing 100191, China; wlx_buaa@163.com (L.W.); guerremondiale@buaa.edu.cn (K.Y.)
[2] Chinese Flight Test Establishment, Xi'an 710089, China; qq645980019@163.com
* Correspondence: yueting_buaa@163.com; Tel.: +86-138-1017-1251

Abstract: For aircraft employing the fly-by-wire technique, the closed-loop dynamic characteristics are determined by both the configuration design and the flight control system. As the capacity of the control system has certain limitations, the configuration parameters are also constrained by the requirements of the closed-loop flying qualities. This paper presents an aircraft configuration parameter boundaries determination method based on closed-loop flying qualities requirements independent of the actual flight control law design, mainly aiming at the parameters that affect the stability and control characteristics. First, a nonlinear dynamic inversion-based flight control law is adopted to decouple the control law gains from the configuration parameters and to study the relationship between the configuration parameters and closed-loop flying qualities. Second, a flying qualities evaluation scheme is established by selecting the most severe flight conditions and the evaluation criteria that are most sensitive to changes in the parameters. Finally, the parameter boundaries according to the requirements of Level 1 flying qualities are determined by searching for the critical values that lead to degradation of the flying qualities. The proposed method is verified by an application example of the design ranges of a sample aircraft's wing position, horizontal tail area, center of gravity, vertical tail area and vertical tail position.

Keywords: configuration design; flying qualities; flight control law

Citation: Wang, L.; Yang, K.; Zhao, P.; Yue, T. Aircraft Configuration Parameter Boundaries Based on Closed-Loop Flying Qualities Requirements. *Aerospace* **2021**, *8*, 360. https://doi.org/10.3390/aerospace8120360

Academic Editors: Dieter Scholz

Received: 1 September 2021
Accepted: 17 November 2021
Published: 24 November 2021

1. Introduction

Aircraft configuration design depends on the design requirements of different types of parameters [1,2]. For example, the determination of wing area, fuselage geometry and cross section mainly considers the payload requirement; the airfoil, aspect ratio and sweep angle of the wing are designed according to the aerodynamic characteristics requirements; wing position, horizontal tail area, center of gravity (CG), vertical tail area and position have considerable influences on the dynamic characteristics of aircraft, and the design of these parameters is conducted mainly in consideration of stability and control requirements [3].

The flying qualities evaluation can comprehensively assess the stability and control characteristics, the performance of the flight control system, and the adaptability to the flight missions [4–8]. Thus, the configuration design should take into account the flying qualities requirements. As the developments of digital flight control systems and the fly-by-wire technique allow more advanced flight control laws (FCL) to be implemented on aircraft [9–15], the configuration design has become more diversified. However, the capacity of FCL has certain limitations, and flying qualities cannot be guaranteed only relying on the control system. Considering that the flying qualities of the closed-loop aircraft are determined by both the configuration design and the flight control system, the configuration parameters are also constrained by the closed-loop flying qualities requirements [16]. Therefore, it is necessary to establish the relationship between the configuration parameters and the closed-loop flying qualities requirements in the conceptual aircraft design.

Recently, there has been renewed interest in the closed-loop flying qualities prediction and assessment in conceptual aircraft design [17–22]. The Institute of Aeronautics and Astronautics of RWTH Aachen University developed a methodology for the prediction and assessment of flying qualities and implemented it into a preliminary aircraft design tool [20]. Arthur Rizzi et al. achieved the multidisciplinary optimization of a canard configured TransCruiser with flight control by using CEASIOM, a multidisciplinary software environment for aircraft design [21]. Stefano Cacciola et al. realized the optimization of the longitudinal control law, as well as the three-surface configuration for better flying qualities [22]; however, the FCLs involved in these studies were mainly stability augmentation systems (SAS) or stability and control augmentation systems (SCAS), which are based on linear control theory and well-established gain-scheduling methods [16]. As a result, the controller gains are coupled with the configuration parameters of the aircraft, and thus, it is impossible to identify the influence of the configuration parameters separately from the influence of the controller gains on the closed-loop flying qualities. Due to this lack of flexibility, the traditional FCLs are not suitable to study the relationship between the configuration parameters and the closed-loop flying qualities requirements.

Inverse model-based control techniques, e.g., nonlinear dynamic inversion (NDI) as well as incremental nonlinear dynamic inversion (INDI), offer a great advantage to continuously changing plants [23,24]. The studies of DLR (German Aerospace Center) and others [25,26] show that the flight control law based on the NDI method can effectively adapt to changing aircraft configurations. Therefore, this paper proposes an aircraft configuration parameter boundaries design method based on closed-loop flying qualities requirements. This method realizes the configuration parameter boundaries design independent of actual flight control law design by using the NDI method, and the closed-loop flying qualities requirements are transformed into the design ranges of target configuration parameters. The parameter boundaries simplify the stability and control design, so that the configuration design can be more focused on aerodynamic, structural and other requirements.

The remainder of this paper is structured as follows. Section 2 introduces the determination method of configuration parameter boundaries based on flying qualities requirements. Section 3 defines the wing position, horizontal tail area, CG position, vertical tail area and vertical tail position as the target configuration parameters. Section 4 describes the modelling of the closed-loop aircraft and proposes the selection of flight conditions and evaluation criteria. An application example comprising the target parameter design of a medium-range transport aircraft is then shown in Section 5. Finally, a concluding summary is given in Section 6.

2. Configuration Parameter Boundaries Based on Flying Qualities Requirements

Conceptual design is the first phase of the aircraft design process. It involves sketching a variety of possible configurations that meet the design requirements, such as aerodynamics, propulsion, flight performance, structural and control systems.

The steps of conceptual design are described as [1,2,27]:

- Preliminary Sizing: definition of requirements, selection of an aircraft configuration, selection of a propulsion system, etc.
- Layout sizing: fuselage sizing, wing sizing, empennage sizing, design for high lift, etc.
- Specific design: stability and control design, flight control system design, landing gear design, structures design, etc.
- Aircraft performance analysis: aerodynamic analysis, polar estimation, mass estimation, flying qualities evaluation, mission analysis, etc.

The whole design process has an iterative nature to realize optimization design [27].

Stability and control design and flying qualities evaluation are often in later stages of the design phase. Configuration parameters adjustment due to stability and control requirements or flying qualities requirements may lead to much iterative work. This paper proposes a method to determine the configuration parameter boundaries based on closed-

loop flying qualities requirements to simplify the stability and control design. The proposed parameter boundaries aim to transform the closed-loop flying qualities requirements into the design ranges of target configuration parameters. In this way, the flying qualities requirements can be considered at the layout sizing stage during optimization design.

The determination process of the parameter boundaries is as follows. The first step is to construct a high-order closed-loop aircraft model according to the basic configuration design; the model can be divided into an aircraft motion model and the FCL based on the model reference NDI method. The second step is to establish the flying qualities evaluation scheme by selecting the most stringent flight conditions and the evaluation criteria that are most sensitive to the parameter changes. The third step is to establish a reasonable variation series of the target parameters and to search for the critical values that lead to degradation of the flying qualities. Finally, the parameter boundaries according to the requirements of the Level 1 flying qualities (Level 1 FQ) are determined. The method for determining parameter boundaries is shown in Figure 1.

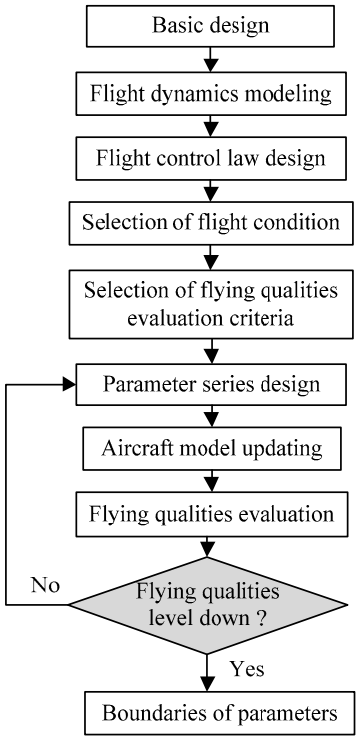

Figure 1. Configuration parameter boundaries based on closed-loop flying qualities requirements.

It should be emphasized that the parameter boundaries proposed in this paper correspond to specific flying qualities criteria, so they only reflect a part of stability and control requirements. Meanwhile, these configuration parameters should also meet other requirements. For example, the CG position design should meet the trim requirements, the vertical tail design should meet the controllability requirements in the single-engine out condition at take-off, and so forth. Designers should seek to reach the design configuration that satisfactorily meets all requirements in the optimization design process.

3. Configuration Parameter Analysis

3.1. Wing Position and Horizontal Tail Area

The longitudinal stability and control characteristics of aircraft are determined mainly by the stability and damping derivatives of the pitch moment, and these derivatives are affected by the wing position, CG position, horizontal tail position, horizontal tail area, and other parameters. The horizontal tail is usually installed at the rear end of the fuselage to ensure the control power of the elevator, and the variation range of the tail position is small.

Thus, the longitudinal characteristics are governed predominantly by the wing position and horizontal tail area [1]. These two parameters are usually designed in collaboration according to the requirements of the longitudinal flying qualities.

The stability derivative of the pitch moment $C_{m\alpha}$ can be expressed as [28]:

$$C_{m\alpha} = C_{L\alpha.WB}\left(x_{c.g.} - x_{ac.WB}\right) - C_{L\alpha.T}V_T + C_{m\alpha.p} \tag{1}$$

where $x_{ac.WB}$ is the mean aerodynamic center of the wing-body configuration and is affected mainly by the wing position; $C_{L\alpha.WB}$ is the lift coefficient derivative of the wing-body configuration; $x_{c.g.}$ is the CG position of the aircraft; $C_{L\alpha.T}$ is the lift coefficient derivative of the horizontal tail; V_T is the horizontal tail volume ratio, affected mainly by the horizontal tail position and its area; and $C_{m\alpha.p}$ is the pitch moment derivative of the propulsion system. V_T is defined as:

$$V_T = \frac{l_T S_T}{cS} \tag{2}$$

where l_T is the distance between the aircraft CG and the aerodynamic center of the horizontal tail, S_T is the horizontal tail area, c is the mean aerodynamic chord of the aircraft wing, and S is the wing area. Consequently, forward movement of the wing position and a decrease in the horizontal tail area lead to a decrease in $|C_{m\alpha}|$ and a reduction in the static longitudinal stability. Similarly, rearward movement of the wing position and an increase in the horizontal tail area lead to an increase in $|C_{m\alpha}|$ and an increase in the demand on the pitch control moment.

The damping derivatives of the pitch moment, namely, C_{mq} and $C_{m\dot{\alpha}}$, are generated mainly by the horizontal tail, whereas the influence of the wing-body configuration accounts for only about 10% of the overall influence [28]. The contributions of the tail to C_{mq} and $C_{m\dot{\alpha}}$ are [28]:

$$\left.\begin{aligned} C_{mq.T} &= -2C_{L\alpha.T}V_T\tfrac{l_T}{c} \\ C_{m\dot{\alpha}.T} &= -2C_{L\alpha.T}V_T\tfrac{l_T}{c}\tfrac{\partial\varepsilon}{\partial\alpha} \end{aligned}\right\} \tag{3}$$

where $\partial\varepsilon/\partial\alpha$ is the derivative of the downwash angle of the horizontal tail with respect to the angle of attack. A decrease in horizontal tail area leads to a decrease in both $\left|C_{mq}\right|$ and $\left|C_{m\dot{\alpha}}\right|$.

The stability and damping derivatives of the pitch moment mainly affect the longitudinal short-period mode characteristics of aircraft. The natural frequency $\omega_{\mathrm{n.sp}}$ and damping ratio ξ_{sp} of the short-period mode can be expressed as:

$$\left.\begin{aligned} \omega_{\mathrm{n.sp}} &= \sqrt{-\left(M_\alpha + M_q Z_\alpha\right)} \\ \xi_{\mathrm{sp}} &= -\frac{M_q + M_{\dot{\alpha}} - Z_\alpha}{2\omega_{\mathrm{n.sp}}} \end{aligned}\right\} \tag{4}$$

where M_α, M_q, $M_{\dot{\alpha}}$, and Z_α are the dimensional dynamic derivatives related to $C_{m\alpha}$, C_{mq}, $C_{m\dot{\alpha}}$ and $C_{L\alpha}$, respectively. The detailed derivation process from (3) to (4) is described in the references [29,30].

Combining Equations (3) and (4) demonstrates that a decrease in the horizontal tail area leads to a decrease in ξ_{sp}, slows down the short-period convergence, and decreases the dynamic stability of the aircraft; in contrast, an increase in the tail area leads to an increase in the damping ratio and restrains the pitch response to the pilot control input.

In a general conceptual design process, the horizontal tail is first of all sized from static conditions as done with the "V-diagram" [27,31,32], which corresponds to the basis of the longitudinal stability and control requirements. Then, the horizontal tail design should consider the dynamic stability and control requirements, which are the primary focus of this paper.

According to the above analysis, the longitudinal dynamic stability requirements of the aircraft should be considered to determine the forward range of the wing position and the maximum limit of the horizontal tail area. Furthermore, the rearward range of the wing position and the minimum limit of the horizontal tail area should be determined by the longitudinal maneuverability requirements.

3.2. Center of Gravity Position

The CG is not a fixed point but moves with the initial loading condition and fuel consumption of the aircraft. For an aircraft with determined aerodynamic shape, a change in the CG position x_{cg} causes $C_{m\alpha}$ to vary and thus affects the longitudinal characteristics. Therefore, the range of the CG location needs to be strictly designed according to the requirements of the longitudinal flying qualities.

A forward CG represents a large $|C_{m\alpha}|$ and requires a larger pitch control moment, while a rearward CG position represents a small $|C_{m\alpha}|$ and poor longitudinal stability. Therefore, in this paper, the forward CG limit mainly considers the longitudinal maneuverability requirements, and the rearward CG limit is determined by the longitudinal stability requirements.

Additionally, the forward CG limit should allow the aircraft to be trimmed at maximum lift coefficient in ground effect. The final forward CG limit will be determined by both the longitudinal maneuverability and trim requirements, which leads to future investigations.

3.3. Vertical Tail Area and Position

Directional stability, also known as weathercock stability, is provided primarily by the vertical tail. Meanwhile, a large vertical tail is accessible spiral stability. However, a large vertical tail surface may produce an excessive aerodynamic drag force during high-speed flight at high altitudes in cruise, and such a large surface would require a higher structural strength and mass of the airframe. Therefore, it is necessary to restrict the vertical tail area to optimize both the aerodynamic characteristics in cruise and the airframe structure. To ensure the directional stability after the vertical tail area is reduced, it is necessary to increase the vertical tail arm by adjusting the position of the vertical tail. Similar to the horizontal tail, the vertical tail is also installed at the end of the fuselage to ensure the control power of the rudder. Thus, the vertical tail position should be adjusted by changing the chord length, sweep angle and other parameters without moving the root position. It should be noted that a large sweep angle may lead to the decrease of the vertical tail lift coefficient. Thus, the vertical tail design should avoid a large sweep angle [29,30].

The contributions of the vertical tail to the stability and damping derivatives of the directional moment $C_{n\beta.V}$ and $C_{nr.V}$ can be expressed as [28]:

$$\left.\begin{aligned} C_{n\beta.V} &= -C_{Y\beta.V} V_V \\ C_{nr.V} &= -2C_{Y\beta.V} V_V \tfrac{l_V}{b} \\ V_V &= \frac{l_V S_V}{bS} \end{aligned}\right\} \tag{5}$$

where $C_{Y\beta.V}$ is the lift coefficient derivative of the vertical tail; V_V is the vertical tail volume ratio; S_V is the vertical tail area; l_V is the force arm of the vertical tail; and b is the wingspan of the aircraft.

The stability and damping derivatives of the directional moment affect mainly the Dutch roll mode characteristics of the aircraft. The natural frequency $\omega_{\mathrm{n.dr}}$ and damping ratio ξ_{dr} of the Dutch roll mode can be expressed as:

$$\left.\begin{aligned} \omega_{\mathrm{n.dr}} &= \sqrt{N_\beta - N_\beta Y_r + N_r Y_\beta} \\ \xi_{\mathrm{dr}} &= -\frac{N_r + Y_\beta}{2\omega_{\mathrm{n.dr}}} \end{aligned}\right\} \tag{6}$$

where N_β, N_r, Y_β, and Y_r are the dimensional dynamic derivatives related to $C_{n\beta}$, C_{nr}, $C_{Y\beta}$ and C_{Yr}, respectively. The detailed derivation process from (5) to (6) is also described in the references [29,30]. Combining Equations (5) and (6) reveals that a reduced vertical tail arm and a decrease in the tail area cause a reduction in both $\left|C_{n\beta}\right|$ and ξ_{dr} and decreases the directional static and dynamic stability.

In a general conceptual design process, vertical tail sizing for static stability has to compensate for the destabilizing effect of the fuselage; vertical tail sizing for static control has to compensate the yaw moment from a one-engine out flight case [29,30]; vertical tail sizing for roll response control requires the proper balance of the rolling time constant and the roll sensitivity; there are also spiral stability and directional dynamic stability requirements. Directional dynamic stability mainly refers to the Dutch roll mode stability, which is the primary focus of this paper. The eventual vertical tail area will be the minimum area that meets all these requirements.

4. Aircraft Modeling, Selection of Flight Conditions and Evaluation Criteria

4.1. Aircraft Modelling

The aircraft motion model is based on the six-degree-of-freedom equations of motion. To determine the configuration parameter boundaries based on closed-loop flying qualities requirements, the motion model should be constantly updated according to the changes in the configuration parameters.

To easily adapt the control laws to continuously change the aircraft configuration during the design process, NDI controllers offer considerable advantages. For instance, the model reference NDI control law [33,34] uses transfer function-based reference models to describe the desired aircraft dynamics. The reference models can be expressed as [33]:

$$\left.\begin{aligned} \frac{q_r}{q_c} &= \frac{K_{q.r}\omega_{\mathrm{sp.r}}^2(s+1/T_{\theta 2.\mathrm{r}})}{s^2+2\xi_{\mathrm{sp.r}}\omega_{\mathrm{sp.r}}s+\omega_{\mathrm{sp.r}}^2} \\ \frac{p_r}{p_c} &= \frac{K_{p.r}}{s+\omega_{p.r}} \\ \frac{r_r}{r_c} &= \frac{\omega_{r.r}}{s+\omega_{r.r}} \end{aligned}\right\} \tag{7}$$

where p_c, q_c, and r_c are the rate commands of the pilot; p_r, q_r, and r_r are the corresponding reference rate commands generated by the reference models; $K_{q.r}$ and $K_{p.r}$ are the control gains; $\xi_{\mathrm{sp.r}}$, $\omega_{\mathrm{sp.r}}$, and $T_{\theta 2.\mathrm{r}}$ are the desired damping ratio, natural frequency and time constant of the short-period mode, respectively; and $\omega_{p.r}$ and $\omega_{r.r}$ are the desired roll and directional frequencies. The reference commands are achieved by the actual dynamic inversion at the core of the control law, which computes the necessary surface positions. A proportional-integral (PI) compensator is added to drive down the error between the desired dynamics and the actual dynamics. Filters are also needed to attenuate undesirable noise from the feedback sensors. The structure of the high-order closed-loop aircraft model with the model reference NDI control law is shown in Figure 2.

The parameters of the model reference NDI control law are designed according to the desired dynamic characteristics and do not need to be adjusted according to changes in the configuration parameters [25]. As a result, the FCL achieves the desired closed-loop flying qualities of the varying aircraft configuration and eliminates the disturbance attributable to variation in the control system. Therefore, the model reference NDI method is employed to design the control law in this paper, which is convenient for studying the relationship between the configuration parameters and the closed-loop flying qualities.

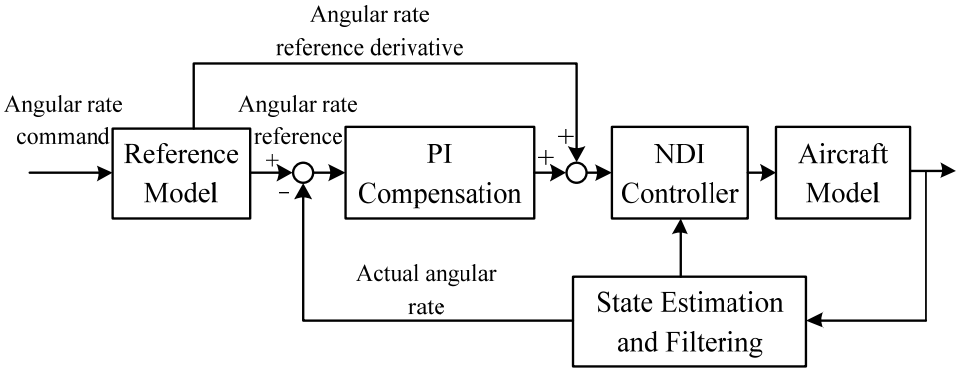

Figure 2. Structure of the high-order closed-loop aircraft model.

It should be emphasized that the design ranges of the configuration parameters derived from the NDI control law represent the capability of control laws that makes the closed-loop aircraft meet the flight quality requirements. For aircraft adopting other control laws, such as SCAS, the conclusions are still valid.

4.2. Selection of Flight Conditions for Evaluation

Any variation in the flight conditions will lead to a change in the flying qualities evaluation results, so the requirements for the configuration parameters differ under different flight conditions. Consequently, to determine configuration parameter boundaries based on closed-loop flying qualities requirements, it is necessary to determine the flight conditions with the most severe requirements for the configuration parameters [1,3].

The previous discussion shows that the forward range of the wing position, the minimum limit of the horizontal tail area, and the rearward CG limit are the main factors influencing the longitudinal dynamic stability requirements of the aircraft. In contrast, the longitudinal maneuverability requirements are governed primarily by the rearward range of the wing position, the maximum limit of the horizontal tail area and the forward CG limit. For aircraft whose load and fuel are arranged mainly in the front region of the airframe, the forward CG limit appears during the take-off phase [1]. In this case, the stability margin of the aircraft is large during the take-off phase, and the longitudinal maneuverability is poor. Considering the low flight speed during the take-off phase, the aerodynamic efficiency of the control surface is low, which worsens the maneuverability. Therefore, the rearward range of the wing position, the maximum limit of the horizontal tail area and the forward CG limit should be determined in the take-off phase. The flight speed, flight altitude, weight distribution, flaps, landing gear and other settings should be consistent with the most forward CG position. With loading and fuel consumption, the CG position reaches the rearward limit in landing phase, during which the stability margin of the aircraft decreases and the most stringent requirements for the longitudinal stability are generated. Therefore, the forward range of the wing position, the minimum limit of the horizontal tail area and the rearward CG limit should be determined in landing phase, and the exact flight condition should be set to the state with the most rearward CG position. The selected flight conditions for evaluating an aircraft whose load and fuel are arranged mainly at the rear of the airframe are the opposite. For an aircraft whose load and fuel cannot be judged clearly whether they are arranged in the front or rear position (for example, the fuel is in the wings and the wingbox), the flight conditions for longitudinal flying qualities evaluation can be selected directly according to the change of the CG position during flight.

The vertical tail design for the directional dynamic stability should be determined under the flight condition with the most stringent requirements. Due to the decrease in damping coefficients during high-speed and high-altitude flight, the Dutch roll mode of the aircraft will deteriorate, thereby increasing the dynamic stability requirements. Therefore, the cruise phase at high speed and high altitude is selected to determine the

design ranges of the vertical tail area and position based on the directional dynamic stability requirements. The exact flight condition should be set to the state with the most decreased damping coefficients.

4.3. Selection of the Flying Qualities Evaluation Criteria

Current flying qualities standards provide multiple evaluation criteria [35–38]. Each evaluation criterion has its own inspection focus, and thus, the same configuration design may yield different evaluation results according to different criteria. To determine configuration parameter boundaries based on closed-loop flying qualities requirements, it is necessary to determine the evaluation criteria that are most sensitive to changes in the configuration parameters to obtain the strictest parameter design ranges.

4.3.1. CAP Criterion

The control anticipation parameter (CAP) is defined as the ratio of the initial pitch acceleration to the steady-state normal acceleration [38]. The CAP value can reflect the short-period mode flying qualities of an aircraft, including the longitudinal stability and maneuverability. To apply the CAP criterion to a high-order closed-loop aircraft, the low-order equivalent system (LOES) theorem is adopted to match the characteristics of the high-order system. The longitudinal LOES of the aircraft can be expressed as:

$$\left.\begin{aligned} \frac{\alpha}{F_e} &= \frac{K_\alpha}{s^2 + 2\zeta_{sp}\omega_{n.sp}s + \omega_{n.sp}^2} e^{-\tau_\alpha s} \\ \frac{q}{F_e} &= \frac{K_q(s + 1/T_{\theta_2})}{s^2 + 2\zeta_{sp}\omega_{n.sp}s + \omega_{n.sp}^2} e^{-\tau_q s} \end{aligned}\right\} \tag{8}$$

where α is the aircraft angle of attack; q is the pitch rate; F_e is the pitch control input; $1/T_{\theta_2}$ is the zero of the pitch attitude transfer function; K_α and K_q are the equivalent system gains of the transfer functions; and τ_α and τ_q are the equivalent time delays.

The CAP of the LOES is defined as:

$$\mathrm{CAP} = \omega_{n.sp}^2 \Big/ \left(\frac{V}{g} \cdot \frac{1}{T_{\theta 2}}\right) \tag{9}$$

where V is the flight speed and g is the acceleration due to gravity. The Level 1 FQ of the CAP criterion are defined by the short-period damping ratio ζ_{sp} of the equivalent system and the CAP value.

The upper boundary of the CAP value and the lower boundary of ζ_{sp} reflect the stability requirements of an aircraft. A large CAP value and small ζ_{sp} indicate a lack of longitudinal stability, and thus, a pilot's small control input may lead to a violent pitch response. Therefore, the upper boundary of the CAP value and the lower boundary of ζ_{sp} can be used to determine the forward range of the wing position, the minimum limit of the horizontal tail area and the rearward CG limit.

In contrast, the lower boundary of the CAP value and the upper boundary of ζ_{sp} reflect the maneuverability requirements. A small CAP value and large ζ_{sp} represent a large longitudinal stability margin, which may increase the pilot's workload to achieve pitch motion. Thus, the rearward range of the wing position, the maximum limit of the horizontal tail area and the forward CG limit should be designed according to the lower boundary of the CAP value and the upper boundary of ζ_{sp}.

4.3.2. Chalk Criterion

The Chalk criterion is a time-domain criterion that focuses on the characteristics of the pitch rate response and defines three parameters for evaluation: the effective time delay t_1, the transient peak ratio $\Delta q_{max}/\Delta q_{min}$ and the effective rise time Δt, as shown in Figure 3 [38].

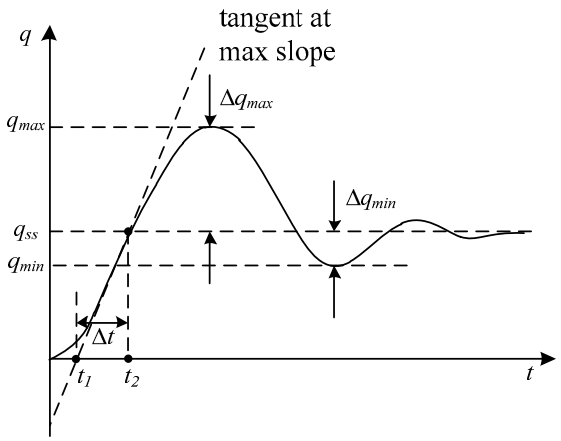

Figure 3. Definitions of the Chalk criterion parameters.

In Figure 3, q_{ss} is the steady-state pitch rate; $q_{\max}$ is the maximum pitch rate; $q_{\min}$ is the first minimum pitch rate; the instant t_1 is defined by the intersection between the tangent at the maximum slope and the time axis; the instant t_2 is defined by the intersection between the tangent at the maximum slope and the horizontal line of the steady-state pitch rate; and Δt is the difference between t_1 and t_2. t_1 reflects the time delay between the real pitch rate response and an ideal pitch rate response with the maximum pitch acceleration, $\Delta q_{\max}/\Delta q_{\min}$ reflects the short-period damping ratio of the pitch response, and Δt reflects the rise time to accelerate to the steady-state pitch rate of the pitch rate ideal response.

The Chalk criterion is based on the time-domain pitch response of the aircraft without identifying the frequency-domain characteristics. Thus, the Chalk criterion can be used to avoid the situation in which a frequency-domain criterion is not applicable to aircraft with an unconventional response. The design ranges of the configuration parameters should be determined according to the more stringent requirements of the CAP and Chalk criteria to enhance the universality of the design method based on closed-loop flying qualities requirements.

4.3.3. Dutch Roll Criterion

The flying qualities with respect to the yaw axis can be evaluated by the characteristics of the lateral-directional oscillatory (Dutch roll) response to the yaw controller. The Dutch roll frequency and damping ratio can be defined by matching the higher-order sideslip response to the yaw control input to the following lower-order form [38]:

$$\frac{\beta}{F_r} = \frac{K_\beta}{(s^2 + 2\xi_{\mathrm{dr}}\omega_{n.\mathrm{dr}}s + \omega_{n.\mathrm{dr}}^2)} e^{-\tau_{e\beta}s} \tag{10}$$

where β is the sideslip angle; F_r is the yaw control input; K_β is the equivalent system gain of the transfer function; and $\tau_{e\beta}$ is the equivalent time delay of the transfer function.

The flying qualities requirements of the Dutch roll criterion are specified in terms of the minimum values of $\omega_{\mathrm{n.dr}}$, ξ_{dr} and $\xi_{\mathrm{dr}}\omega_{\mathrm{n.dr}}$, and the evaluation results can reflect the lateral-directional stability of the aircraft. This criterion can be used to determine the vertical tail area and position boundaries.

5. Application of the Proposed Parameter Boundaries Design Method

This section takes a medium-range transport aircraft as an application example of the configuration parameter boundaries design method. The definitions of the target configuration parameters of the sample aircraft are illustrated in Figure 4. The wing position x_W and the vertical tail position x_V are defined as the distance from the nose to the quarter chord point on the mean aerodynamic chord (MAC) of the wing and the vertical

tail. The CG position $\overline{x}_{cg}$ is defined as the percentage of the distance from the CG to the leading edge of the wing MAC [1].

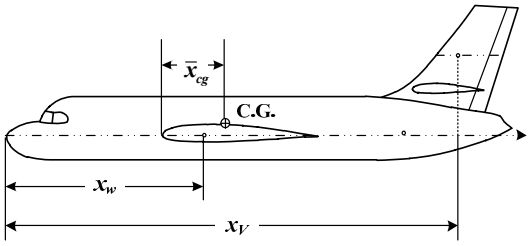

Figure 4. Target configuration parameters of the sample aircraft.

The configuration parameters of the basic aircraft design are depicted in Table 1. The aircraft motion model and the inner loop of the NDI control law are based on the basic aircraft design, and the reference model parameters of the NDI control law are designed according to the flying qualities requirements, as shown in Table 2. By combining the motion model with the FCL, the high-order closed-loop aircraft model is established.

Table 1. Configuration parameters of the basic aircraft design.

Parameters	Values
Length overall (m)	32
Wing position (m)	12.6
Wing area (m^2)	115.3
Wing mean aerodynamic chord (MAC) (m)	6.2
Center of gravity	33.4% (TO) 38.2% (LD)
Horizontal tail position (m)	28.6
Horizontal tail area (m^2)	27.5
Horizontal tail MAC (m)	2.9
Vertical tail position (m)	29.8
Vertical tail area (m^2)	15.9
Vertical tail MAC (m)	3.2

Table 2. Reference model parameters design.

$K_{q.r}$	$\xi_{\mathbf{sp.r}}$	$\omega_{\mathbf{sp.r}}$ (rad/s)	$T_{\theta 2.\mathbf{r}}$ (s)	$K_{p.r}$	$\omega_{p.r}$ (rad/s)	$\omega_{r.r}$ (rad/s)
7.5	0.9	3.5	0.5	4.2	2.5	3.5

5.1. Boundaries of the Wing Position and Horizontal Tail Area

For the sample aircraft, the forward CG limit appears in the take-off phase (sea-level, low-speed, forward CG position, maximum take-off weight, maximum thrust, flaps and landing gear retracted), while the rearward CG limit appears in the landing phase (sea-level, low-speed, rearward CG position, minimum landing weight, landing engine setting, flaps and landing gear down). According to the previous discussion, the forward range of x_W and the minimum limit of S_T should be designed by evaluating the flying qualities in landing phase according to the most stringent requirement among the upper boundary of the CAP value, the lower boundary of ξ_{sp}, and the Chalk criterion. Likewise, the rearward range of x_W and the maximum limit of S_T should be designed in take-off phase according to the most stringent requirement among the lower boundary of the CAP value, the upper boundary of ξ_{sp} and the Chalk criterion.

Preliminary sizing requires that the CG position is on the MAC of the wing; thus, the first estimate of x_W ranges from 10 m to 16 m. Then, according to the requirements of the longitudinal Level 1 FQ of closed-loop aircraft, the design range of S_T corresponding to different x_W is determined. Since the rearward range of x_W and the maximum limit of S_T both reflect the maneuverability requirements, the upper boundary of S_T corresponding to

different x_W can also be regarded as the rearward boundary x_W corresponding to different S_T. Similarly, the lower boundary of S_T corresponding to different x_W can also be regarded as the forward boundary of x_W corresponding to different S_T. The design range of x_W is determined by the design range of S_T.

- Maximum limit of the horizontal tail area

The variation series of x_W is established as follows: within the preliminary range from 10 m to 16 m, one point is selected every 1 m, yielding seven points in total. For each X_W, a series of S_T with an interval of 2 m^2 is selected. Then, the CAP criterion is applied to evaluate the flying qualities of aircraft with different x_W–S_T combinations in the take-off phase. Partial evaluation results with x_W values of 10 m, 12 m, 14 m, and 16 m are shown in Figure 5. The CAP criterion characteristics with x_W values of 12 m and 14 m are shown in Table 3.

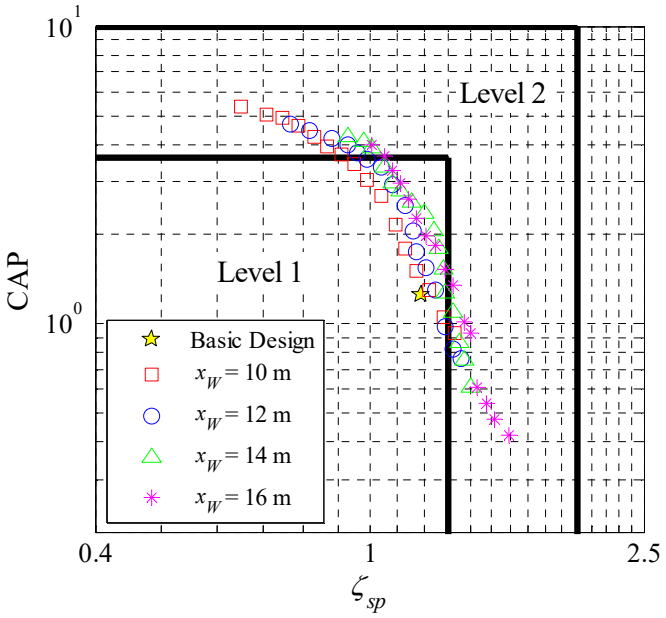

Figure 5. CAP criterion evaluation results in take-off phase.

Table 3. CAP criterion evaluation results with x_W = 12 m and 14 m in the take-off phase.

x_W (m)	S_T (m^2)	ξ_{sp}	CAP	Level	x_W (m)	S_T (m^2)	ξ_{sp}	CAP	Level
12	18	0.96	3.76	2	14	14	1.01	3.87	2
12	20	0.99	3.56	1	14	16	1.05	3.35	1
12	22	1.04	3.35	1	14	18	1.08	2.96	1
12	24	1.08	2.92	1	14	20	1.11	2.79	1
12	26	1.13	2.49	1	14	22	1.15	2.57	1
12	28	1.16	2.06	1	14	24	1.20	2.36	1
12	30	1.17	1.75	1	14	26	1.24	2.05	1
12	32	1.21	1.55	1	14	28	1.26	1.79	1
12	34	1.25	1.29	1	14	30	1.28	1.52	1
12	36	1.29	0.98	1	14	32	1.29	1.27	1
12	38	1.32	0.82	2	14	34	1.32	1.09	2

For a certain x_W, the CAP value decreases gradually with increasing S_T, and the damping ratio ξ_{sp} increases. The maximum limit of S_T defined by the CAP criterion is the critical value that leads to the degradation of the flying qualities to Level 2. When x_W is set to 12 m and 14 m, the corresponding maximum limit of S_T is 36 m^2 and 32 m^2, respectively. Hence, as the wing position moves rearward, the maximum limit of S_T gradually decreases.

According to all the above evaluation results, the level boundaries of the x_W–S_T combination defined by the CAP criterion in take-off phase are presented in Figure 6.

According to this figure, to ensure the Level 1 FQ of the CAP criterion, when x_W is set as 10 m, the corresponding design range of S_T is from 24 m^2 to 38 m^2; when x_W is set as 16 m, the S_T design range is from 14 m^2 to 26 m^2. The right boundary of Level 1 in Figure 6 determines the maximum limit of S_T corresponding to different x_W, and the rearward range of x_W corresponding to different S_T.

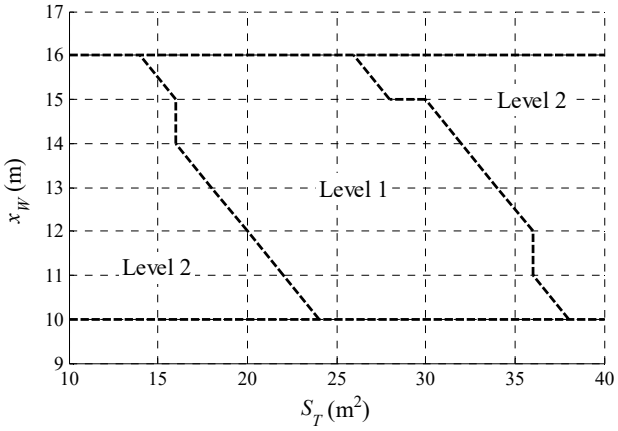

Figure 6. Parameter level boundaries defined by the CAP criterion in the take-off phase.

The Chalk criterion is also applied to evaluate the flying qualities in the take-off phase. Figure 7 shows the influence of changing S_T on the pitch rate response with x_W = 12 m. The variations in the tail area exert the main influences on the response peak and response speed of the pitch rate. As S_T increases, the response peak decreases, and the response time delay increases. The influence of the rearward displacement of the wing is similar to that of changing S_T, which means that decreasing x_W will reduce both the response peak and the response speed.

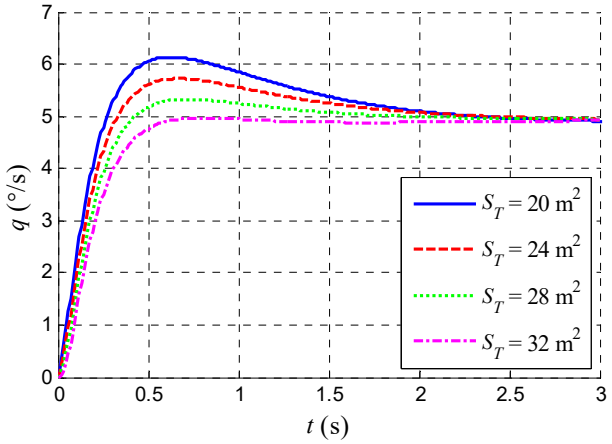

Figure 7. Pitch rate responses with different S_T.

Among all Chalk criterion parameters, the effective time delay t_1 is the most affected by the variations in and S_T. The evaluation results of t_1 are shown in Table 4. The transient peak ratio $\Delta q_{max}/\Delta q_{min}$ and the effective rise time Δt are also affected, but the FQ Level is not degraded. With the rearward movement of the wing and an increase in the tail area, the t_1 of the pitch response increases, which indicates poor maneuverability. The FQ Level is degraded to Level 2 (0.12 s < t_1 < 0.17 s) or even Level 3 (t_1 > 0.17 s). In the chosen ranges of x_W and S_T, an increase in x_W and a decrease in S_T will not degrade the flying qualities of the Chalk criterion.

Table 4. Chalk criterion evaluation results in the take-off phase (t_1, seconds).

S_T (m^2) / xw (m)	18	20	22	24	26	28	30	32	34	36	38	40
10	0.049	0.055	0.065	0.071	0.076	0.083	0.091	0.098	0.107	0.112	0.118	0.129
11	0.055	0.063	0.072	0.082	0.082	0.095	0.103	0.105	0.109	0.115	0.125	0.137
12	0.063	0.071	0.081	0.091	0.089	0.102	0.109	0.109	0.112	0.118	0.132	0.152
13	0.075	0.079	0.089	0.098	0.095	0.107	0.112	0.113	0.117	0.142	0.156	0.169
14	0.081	0.087	0.095	0.103	0.106	0.113	0.116	0.118	0.135	0.158	0.171	0.182
15	0.092	0.096	0.101	0.109	0.112	0.118	0.128	0.145	0.152	0.167	0.185	0.196
16	0.098	0.102	0.107	0.115	0.119	0.129	0.142	0.155	0.163	0.172	0.192	0.212
Background	Level 1					Level 2			Level 3			

The level boundaries of the x_W–S_T combination defined by the Chalk criterion in the take-off phase are shown in Figure 8. According to this figure, to ensure the Level 1 FQ of the Chalk criterion, the maximum limit of S_T is 38 m^2 when x_W = 10 m, and the maximum limit is 26 m^2 when x_W = 16 m. Compared with the parameter boundaries defined by the CAP criterion shown in Figure 6, the Chalk criterion defines a more relaxed Level 1 boundary of the rearward range of x_W and the maximum limit of S_T. In contrast, the Level 2 boundary defined by the Chalk criterion is stricter and can be used as a supplement to the CAP criterion boundaries.

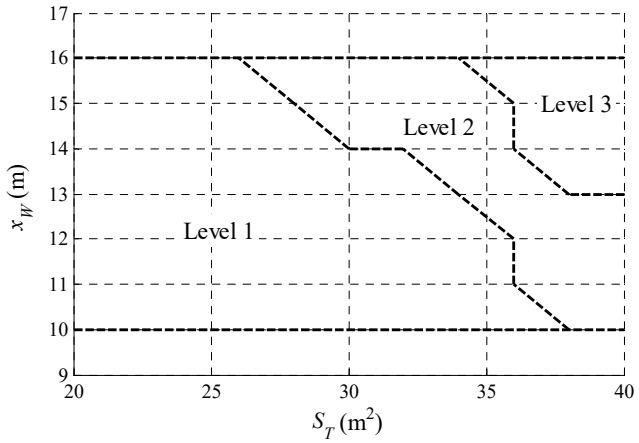

Figure 8. Parameter level boundaries defined by the Chalk criterion in the take-off phase.

- Minimum limit of the horizontal tail area

The selection of the x_W and S_T series is the same as the design of the maximum S_T range. The CAP criterion is applied to evaluate the flying qualities in the landing phase. Partial evaluation results with x_W values of 10 m, 12 m, 14 m, and 16 m are shown in Figure 9, where the corresponding minimum limits of S_T are 26 m^2, 22 m^2, 20 m^2, and 16 m^2, respectively. As the wing position moves forward, the minimum limit of S_T gradually increases.

The level boundaries of the x_W–S_T combination defined by the CAP criterion in landing phase are shown in Figure 10. According to this figure, to ensure the Level 1 FQ of the CAP criterion, the design range of S_T is from 26 m^2 to 40 m^2 when x_W = 10 m and from 16 m^2 to 32 m^2 when x_W = 16 m. The left boundary of Level 1 in Figure 10 can determine the minimum limit of S_T corresponding to different x_W, and the forward range of x_W corresponding to different S_T.

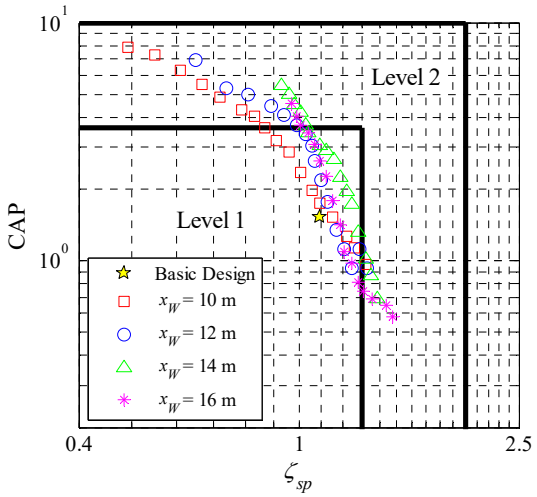

Figure 9. CAP criterion evaluation results in the landing phase.

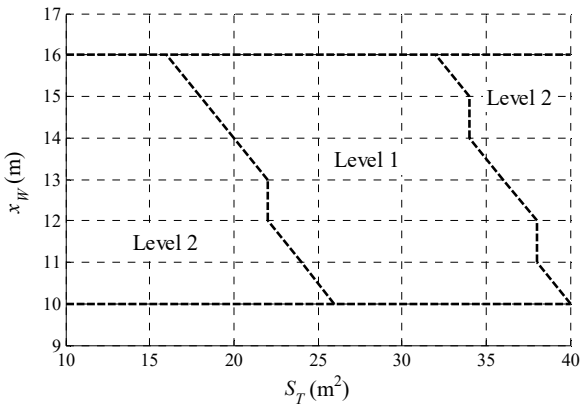

Figure 10. Parameter level boundaries defined by the CAP criterion in the landing phase.

According to the evaluation results of the Chalk criterion in the landing phase, the effective rise time and the response time delay decrease as the wing moves forward and the tail area decreases, which represents a better response speed of the pitch rate. Meanwhile, the pitch damping characteristics become worse as the transient peak ratio $\Delta q_{\max}/\Delta q_{\min}$ increases, but the FQ Level is not degraded. Therefore, the forward boundary of x_W and the minimum limit of S_T should be determined only by the CAP criterion.

- Level boundaries of the wing position and horizontal tail area

To determine the design ranges of x_W and S_T according to the Level 1 FQ requirements in the entire flight envelope, the most stringent boundaries in Figures 6, 8 and 10 are combined to form the final parameter level boundary diagram, as shown in Figure 11.

According to Figure 11, the Level 1 boundary of the rearward x_W and the maximum S_T (right side in Figure 11) is determined by the evaluation results in the take-off phase; the upper half is defined by the Chalk criterion and the lower half is defined by the CAP criterion. The Level 2 boundary (top right in Figure 11) is determined in take-off phase by the Chalk criterion. The Level 1 boundary of the forward x_W and the minimum S_T (left side in Figure 11) is defined in the landing phase by the CAP criterion. The design range of S_T determined by the Level 1 FQ requirements is from 26 m^2 to 38 m^2 when x_W = 10 m and from 16 m^2 to 26 m^2 when x_W = 16 m. In the configuration design process, the design range of S_T can be defined as the horizontal interval within the Level 1 zone (shaded part in Figure 11) corresponding to the designed x_W. Similarly, the design range of x_W is defined as the vertical interval within the Level 1 zone according to the designed S_T.

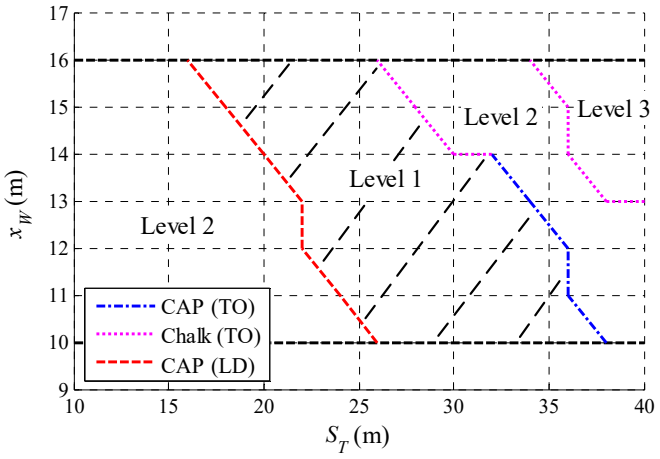

Figure 11. Complete level boundaries of x_W and S_T.

5.2. Boundaries of the Center of Gravity Position

The forward limit of $\overline{x}_{cg}$ should be designed in the take-off phase according to the most stringent requirement among the lower boundary of the CAP value, the upper boundary of ξ_{sp}, and the Chalk criterion. Likewise, the rearward limit of $\overline{x}_{cg}$ should be designed by evaluating the flying qualities in the landing phase according to the most stringent requirement among the upper boundary of the CAP value, the lower boundary of ξ_{sp}, and the Chalk criterion.

The series for the forward $\overline{x}_{cg}$ limit design is set as follows: from 6% to 36%, a point is selected every 3% of the wing MAC, yielding ten points in total. Likewise, the series for the rearward $\overline{x}_{cg}$ limit design is set as follows: from 38% to 65%, a point is selected every 3% of the wing MAC, also yielding ten points in total. Then, the CAP criterion is applied to evaluate the flying qualities of the aircraft with the forward $\overline{x}_{cg}$ in the take-off phase, while the rearward $\overline{x}_{cg}$ designs are evaluated in the landing phase. The evaluation results are presented in Figure 12. Compared with the basic design of the sample aircraft in the take-off phase, as the CG position moves forward (TO phase, $\overline{x}_{cg}$–), the CAP value decreases gradually, the damping ratio ξ_{sp} increases, and the FQ Level is degraded from Level 1 to Level 2. In the landing phase, as the CG position moves rearward (LD phase, $\overline{x}_{cg}$+), the CAP value increases, and the damping ratio ξ_{sp} decreases.

The forward $\overline{x}_{cg}$ designs are also evaluated by the Chalk criterion in the take-off phase. The effective time delay t_1 is the parameter most affected by the variation in $\overline{x}_{cg}$; the evaluation results of t_1 are shown in Table 5. As CG moves forward, the t_1 value of the pitch response increases, which indicates poor maneuverability. The FQ Level is degraded to Level 2 or even Level 3.

Table 5. Chalk criterion evaluation results of the forward $\overline{x}_{cg}$ (t_1, seconds).

$\overline{x}_{cg}$ (% MAC)	t_1 (s)	Level	$\overline{x}_{cg}$ (% MAC)	t_1 (s)	Level
33	0.05	1	18	0.121	2
30	0.061	1	15	0.137	2
27	0.074	1	12	0.155	2
24	0.088	1	9	0.172	3
21	0.103	1	6	0.189	3

According to the evaluation results of the Chalk criterion in the landing phase, the pitch damping characteristics of the aircraft become worse as the CG moves rearward, but the FQ Level is not degraded. Therefore, the Chalk criterion is only applied to design the forward $\overline{x}_{cg}$ limit.

The level boundaries of $\overline{x}_{cg}$ are defined as in Figure 13. According to this figure, the Level 1 boundary of the forward CG limit is 21% of the wing MAC, determined by the

upper boundary of ξ_{sp} in the CAP criterion in the take-off phase. The Level 2 boundary of the forward CG limit is 12% of the wing MAC, determined by the Chalk criterion. Finally, the Level 1 boundary of the rearward CG limit is 59% of the wing MAC, determined by the upper boundary of the CAP value in the landing phase. The $\overline{x}_{cg}$ range should be kept within the Level 1 zone (shaded part in Figure 13).

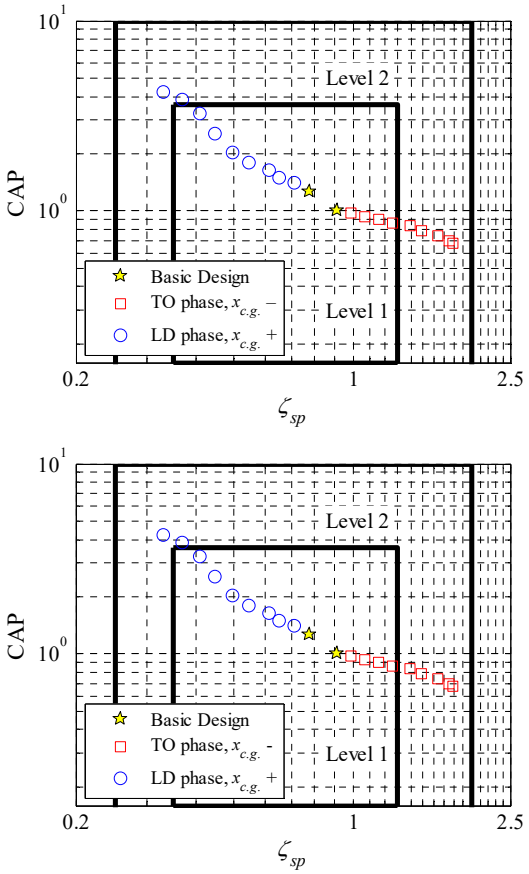

Figure 12. CAP criterion evaluation results of $\overline{x}_{cg}$.

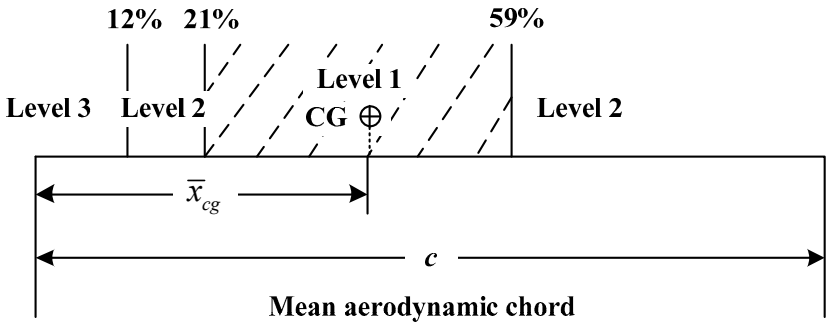

Figure 13. Level boundaries of $\overline{x}_{cg}$.

5.3. Boundaries of the Vertical Tail Area and Position

The vertical tail area S_V and position x_V should be designed in the cruise phase (high speed, high altitude, cruise engine setting and configuration) according to the requirements of the Dutch roll criterion. The variation series of S_V is set as follows: below the basic value of S_V, a point is selected every 1 m^2, and for each S_V, a series of x_V with an interval of 1 m is selected. As x_V is adjusted by changing the quarter chord point of the vertical tail without moving the root position, the design range of x_V is limited from 26 m to 31 m.

Then, the Dutch roll criterion is applied to evaluate the flying qualities of different S_V–x_V combinations. Partial evaluation results with S_V values of 10 m^2, 12 m^2, 14 m^2, and 16 m^2 are shown in Figure 14, and the Dutch roll characteristics with S_V values of 12 m^2 and 14 m^2 are shown in Table 6.

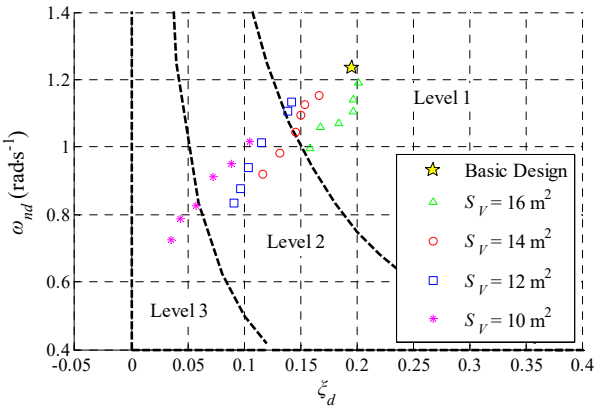

Figure 14. Dutch roll criterion evaluation results in the cruise phase.

Table 6. Dutch roll criterion evaluation results with x_W = 12 m, 14 m in the cruise phase.

S_V (m^2).	x_V (m)	ξ_{dr}	$\omega_{n.dr}$ (rad/s)	Level	S_V (m^2)	x_V (m)	ξ_{dr}	$\omega_{n.dr}$ (rad/s)	Level
12	31	0.142	1.132	1	14	31	0.166	1.153	1
12	30	0.138	1.107	1	14	30	0.154	1.127	1
12	29	0.115	1.012	2	14	29	0.150	1.093	1
12	28	0.104	0.937	2	14	28	0.145	1.044	1
12	27	0.097	0.878	2	14	27	0.132	0.981	2
12	26	0.091	0.835	2	14	26	0.117	0.920	2

For a certain S_V, both $\omega_{n.dr}$ and ξ_{dr} of the Dutch roll mode decrease gradually with the forward movement of the tail. The forward range of x_V is defined as the critical value that leads to the degradation of directional flying qualities. When S_V is set as 12 m^2 and 14 m^2, the corresponding forward range of x_V is 30 m and 28 m, respectively. With decreasing S_V, the design range of x_V gradually decreases. The minimum limit of S_V is defined as the critical value without the corresponding x_V that meets the requirements of the Level 1 FQ.

According to all evaluation results, the level boundaries of the S_V–x_V combination are defined as in Figure 15.

Considering that the drag force due to the vertical tail is largely related to the vertical tail area, it is necessary to restrict the tail area while satisfying the flying qualities requirements. According to Figure 15, x_V within the design range can ensure Level 1 FQ of the closed-loop aircraft when S_V is not less than 15 m^2. The minimum limit of S_V is 11 m^2 and the corresponding x_V is 31 m. In the configuration design process, the design range of S_V can be defined as the horizontal interval within the shaded Level 1 zone in Figure 15, corresponding to the designed x_V. Similarly, the design range of x_V is defined as the vertical interval within the Level 1 zone according to the designed S_V.

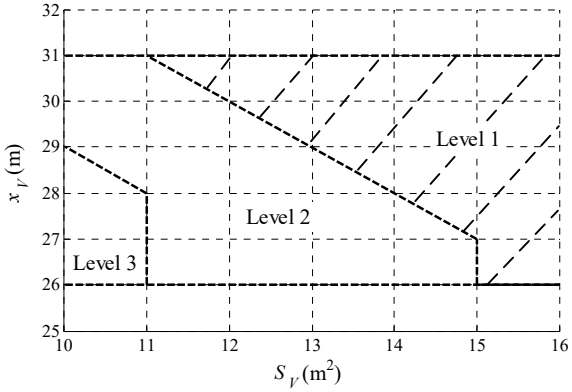

Figure 15. Complete level boundaries of S_V and x_V.

6. Conclusions

In this study, the influences of typical configuration parameters on flying qualities are analyzed, and a configuration parameter boundaries design method based on closed-loop flying qualities requirements is proposed and verified by an application example.

(1) Five typical configuration parameters that should be designed based on flying qualities requirements are determined: wing position, horizontal tail area, center of gravity position, vertical tail area and position.

(2) The proposed configuration parameter boundaries design method based on closed-loop flying qualities requirements is achieved as follows. First, the flight control law is designed based on the model reference nonlinear dynamic inversion method, and a high-order closed-loop aircraft model is established. Second, the most stringent flight conditions and the evaluation criteria that are most sensitive to the target parameters are determined. Third, by searching for the critical values that lead to the degradation of flying qualities, the closed-loop flying qualities requirements are transformed into the design ranges of target configuration parameters.

(3) An application example involving the typical parameter boundaries design of a sample aircraft is provided. The wing position of the sample aircraft ranges from 10 m to 16 m, the design range of the horizontal tail area corresponding to the forward limit of wing position is from 26 m^2 to 38 m^2, and the horizontal tail area range corresponding to the rear limit of wing position is from 16 m^2 to 26 m^2. The design ranges of the wing position and horizontal tail area are defined by the level boundary diagram. The forward limit of the center of gravity is 21% of the average aerodynamic chord, while the rearward limit is 59%. The minimum limit of the vertical tail area is 11 m^2, and the design ranges of the vertical tail area and position are defined by the level boundary diagram.

Author Contributions: Conceptualization, L.W. and K.Y.; methodology, L.W.; software, K.Y.; validation, L.W., K.Y. and T.Y.; formal analysis, K.Y.; investigation, K.Y.; resources, P.Z.; data, P.Z.; writing—original draft preparation, K.Y. and T.Y.; writing—review and editing, T.Y.; project administration, L.W. All authors have read and agreed to the published version of the manuscript.

Funding: This work was supported in part by the Fundamental Funds for the Central Universities of China under Grant YWF-19-BJ-J322.

Institutional Review Board Statement: Not applicable.

Informed Consent Statement: Not applicable.

Data Availability Statement: The high-order closed-loop aircraft model (Figure 2) and data presented in this study can be obtained from the corresponding author on request.

Acknowledgments: The authors would like to deliver their sincere thanks to the editors and anonymous reviewers.

Conflicts of Interest: The authors declare no conflict of interest.

Abbreviations:

CG	Center of Gravity
FCL	Flight Control Laws
SAS	Stability Augmentation System
SCAS	Stability and Control Augmentation System
NDI	Nonlinear Dynamic Inversion
INDI	Incremental Nonlinear Dynamic Inversion
FQ	Flying Qualities
PI	Proportional-Integral
CAP	Control Anticipation Parameter
LOES	Low-Order Equivalent System
MAC	Mean Aerodynamic Chord
TO	Take-Off
LD	Landing

References

1. Raymer, D.P. *Airplane Design: A Conceptual Approach*, 2nd ed.; American Institute of Aeronautics and Astronautics, Inc.: Washington, DC, USA, 1989; ISBN 0-930403-51-7.
2. Anton, E.; Lammering, T.; Henke, R. Fast estimation of top-level aircraft requirement impact on conceptual aircraft designs. In Proceedings of the 10th AIAA Aviation Technology, Integration, and Operations (ATIO) Conference, Fort Worth, TX, USA, 13–15 September 2010. [CrossRef]
3. Cook, M.V. *Flight Dynamics Principles: A Linear Systems Approach to Aircraft Stability and Control*, 2nd ed.; Butter-worth-Heinemann: Burlington, NJ, USA, 1997; ISBN 978-0-7506-6927-6.
4. Wang, L.; Yin, H.; Guo, Y.; Yue, T.; Jia, X. Closed-loop motion characteristic requirements of receiver aircraft for probe and drogue aerial refueling. *Aerosp. Sci. Technol.* **2019**, *93*, 105293. [CrossRef]
5. Campos, L.M.B.C.; Marques, J.M.G. On the Handling Qualities of Two Flying Wing Aircraft Configurations. *Aerospace* **2021**, *8*, 77. [CrossRef]
6. Nicolosi, F.; De Marco, A.; Vecchia, P.D. Stability, flying qualities and longitudinal parameter estimation of a twin-engine CS-23 certified light aircraft. *Aerosp. Sci. Technol.* **2013**, *24*, 226–240. [CrossRef]
7. Wang, L.; Guo, Y.; Zhang, Q.; Yue, T. Suggestion for aircraft flying qualities requirements of a short-range air combat mission. *Chin. J. Aeronaut.* **2017**, *30*, 881–897. [CrossRef]
8. Wang, L.; Xu, Z.; Yue, T. Dynamic characteristics analysis and flight control design for oblique wing aircraft. *Chin. J. Aeronaut.* **2016**, *29*, 1664–1672. [CrossRef]
9. Schulze, M.; Neumann, J.; Klimmek, T. Parametric Modeling of a Long-Range Aircraft under Consideration of Engine-Wing Integration. *Aerospace* **2020**, *8*, 2. [CrossRef]
10. Zhu, J. A survey of advanced flight control theory and application. In Proceedings of the Multiconference on Computational Engineering in Systems Applications, Beijing, China, 4–6 October 2006. [CrossRef]
11. Bauer, C.; Lagadec, K.; Bès, C.; Mongeau, M. Flight Control System Architecture Optimization for Fly-By-Wire Airliners. *J. Guid. Control. Dyn.* **2007**, *30*, 1023–1029. [CrossRef]
12. Zhao, X.; Guerrero, J.M.; Wu, X. Review of aircraft electric power systems and architectures. In Proceedings of the International Energy Conference, Dubrovnik, Croatia, 13–16 May 2014; Available online: https://core.ac.uk/reader/60556259 (accessed on 15 November 2021).
13. Zhu, Z.; Guo, H.; Ma, J. Aerodynamic layout optimization design of a barrel-launched UAV wing considering control capability of multiple control surfaces. *Aerosp. Sci. Technol.* **2019**, *93*, 105297. [CrossRef]
14. Sanchez-Carmona, A.; Cuerno-Rejado, C. Design Process and Environmental Impact of Unconventional Tail Airliners. *Aerospace* **2021**, *8*, 175. [CrossRef]
15. Attar, M.; Wahnon, E.; Chaimovitz, D. Advanced Flight Control Technologies for UAVs. In Proceedings of the 2nd AIAA Unmanned Unlimited Conf. and Workshop & Exhibit, San Diego, CA, USA, 15–18 September 2003. [CrossRef]
16. Brockhaus, R. *Flugregelung*; Springer: Berlin/Heidelberg, Germany, 2001; ISBN 978-3-662-07265-3.
17. Kim, J.P.; Kunz, D.L. Handling Qualities Assessment of an Unmanned Aircraft Using Performance and Workload Metrics. *J. Guid. Control. Dyn.* **2017**, *40*, 1–9. [CrossRef]
18. Humphreys-Jennings, C.; Lappas, I.; Sovar, D.M. Conceptual Design, Flying, and Handling Qualities Assessment of a Blended Wing Body (BWB) Aircraft by Using an Engineering Flight Simulator. *Aerospace* **2020**, *7*, 51. [CrossRef]
19. Liu, F.; Wang, L.; Tan, X. Digital virtual flight testing and evaluation method for flight characteristics airworthiness compliance of civil aircraft based on HQRM. *Chin. J. Aeronaut.* **2014**, *28*, 112–120. [CrossRef]
20. Risse, K.; Anton, E.; Henke, R. Methodology for Flying Qualities Prediction and Assessment in Preliminary Aircraft Design. In Proceedings of the 10th AIAA Aviation Technology, Integration, and Operations (ATIO) Conference, Fort Worth, TX, USA, 13–15 September 2010. [CrossRef]

21. Rizzi, A.; Eliasson, P.; Goetzendorf-Grabowski, T.; Vos, J.B.; Zhang, M.; Richardson, T.S. Design of a canard configured TransCruiser using CEASIOM. *Prog. Aerosp. Sci.* **2011**, *47*, 695–705. [CrossRef]
22. Cacciola, S.; Riboldi, C.E.D.; Arnoldi, M. Three-Surface Model with Redundant Longitudinal Control: Modeling, Trim Optimization and Control in a Preliminary Design Perspective. *Aerospace* **2021**, *8*, 139. [CrossRef]
23. Sonneveldt, L.; Van Oort, E.R.; Chu, Q.; Mulder, J.A. Nonlinear adaptive flight control law design and handling qualities evaluation. In Proceedings of the Joint 48h IEEE Conference on Decision and Control and 28th Chinese Control Conference, Shanghai, China, 15–18 December 2009. [CrossRef]
24. Samadikhoshkho, Z.; Ghorbani, S.; Janabi-Sharifi, F.; Zareinia, K. Nonlinear control of aerial manipulation systems. *Aerosp. Sci. Technol.* **2020**, *104*, 105945. [CrossRef]
25. Hasan, Y.J.; Flink, J.; Freund, S.; Klimmek, T.; Kuchar, R.; Liersch, C.M.; Looye, G.; Moerland, E.; Pfeiffer, T.; Schrader, M.; et al. Stability and Control Investigations in Early Stages of Aircraft Design. In Proceedings of the 2018 Applied Aerodynamics Conference, Atlanta, GA, USA, 25–29 June 2018. [CrossRef]
26. Ji, C.-H.; Kim, C.-S.; Kim, B.-S. A Hybrid Incremental Nonlinear Dynamic Inversion Control for Improving Flying Qualities of Asymmetric Store Configuration Aircraft. *Aerospace* **2021**, *8*, 126. [CrossRef]
27. Scholz, D. *Aircraft Design, Lecture Notes*; Hamburg University of Applied Sciences: Hamburg, Germany, 2015; Available online: http://hoou.ProfScholz.de (accessed on 15 November 2021).
28. Etkin, B.; Teichmann, T. *Dynamics of Flight: Stability and Control*; John Wiley & Sons, Inc.: New York, NY, USA, 1996; ISBN 0-471-03418-5.
29. Scholz, D. *Flight Dynamics, Stability and Control, Lecture Notes*; Hamburg University of Applied Sciences: Hamburg, Germany, 2003; Available online: https://perma.cc/4GHQ-SP33 (accessed on 15 November 2021).
30. McRuer, D.; Ashkenas, I.; Graham, D. *Aircraft Dynamics and Automatic Control*; Princeton University Press: Princeton, NJ, USA, 1973; Available online: https://perma.cc/G9GQ-GJAD (accessed on 15 November 2021).
31. Scholz, D. Empennage sizing with the tail volume complemented with a method for dorsal fin layout. *INCAS Bull.* **2021**, *13*, 149–164. [CrossRef]
32. Barua, P.; Sousa, T.; Scholz, D. *Empennage Statistics and Sizing Methods for Dorsal Fins*; Hamburg University of Applied Sciences: Hamburg, Germany, 2013; Available online: http://purl.org/AERO/TN2013-04-15 (accessed on 15 November 2021).
33. Miller, C.J. Nonlinear Dynamic Inversion Baseline Control Law: Architecture and Performance Predictions. In Proceedings of the AIAA Guidance, Navigation, and Control Conference, Portland, OR, USA, 8–11 August 2011; Available online: https://core.ac.uk/reader/10562991 (accessed on 15 November 2021).
34. Miller, C.J. Nonlinear Dynamic Inversion Baseline Control Law: Flight-Test Results for the Full-scale Advanced Systems Testbed F/A-18 Airplane. In Proceedings of the AIAA Guidance, Navigation, and Control Conference, Portland, OR, USA, 8–11 August 2011; Available online: https://core.ac.uk/reader/10562995 (accessed on 15 November 2021).
35. Harper, R.P.; Cooper, G.E. Handling qualities and pilot evaluation. *J. Guid. Control. Dyn.* **1986**, *9*, 515–529. [CrossRef]
36. United States Department of Defense. *MIL-F-8785, Military Specification, Flying Qualities of Piloted Airplanes*; United States Department of Defense: Arlington, TX, USA, 1980; Available online: https://perma.cc/FN56-6YAG (accessed on 15 November 2021).
37. United States Department of Defense. *MIL-STD-1797A, Military Standard, Flying Qualities of Piloted Aircraft*; United States Department of Defense: Arlington, TX, USA, 1990; Available online: https://perma.cc/EVM7-RW6Z (accessed on 15 November 2021).
38. United States Department of Defense. *MIL-HDBK-1797, Military Standard, Flying Qualities of Piloted Aircraft*; United States Department of Defense: Arlington, TX, USA, 2004; Available online: https://perma.cc/978D-RJFG (accessed on 15 November 2021).